TiO_2 Thin Films by Solution Technique for Solar Cells

Charles Mogunde [1], **Cliff Orori Mosiori** [2]

[1] *Kenyatta University*
P. O. Box 43844-00100, Nairobi, Kenya

[2] *Technical University of Mombasa*
P.O. Box 90420- 80100, Mombasa, Kenya

DOI: 10.22178/pos.37-1

LCC Subject Category: TP155-156

Received 20.06.2018
Accepted 20.07.2018
Published online 31.08.2018

Corresponding Author:
Charles Mogunde
mogundecharles@gmail.com

Abstract. Titanium dioxide has a number of applications in solar cells. In this study, TiO_2 thin films were synthesized using a simple but less expensive, low temperature and large area deposition method referred to as chemical bath deposition. Their electrical and optical properties were examined at various temperatures where it was observed that the films exhibited low reflectance which increased with increase in wavelength with refractive indices of 2.2–2.5 in the visible spectra. Sheet resistivity ranged between 13.54±0.095 Ω/m to 17.27±0.209 Ω/m. They were use to fabricate photovoltaic cell which exhibited the following parameters: a short circuit current, I_{sc}=0.002445 A, open voltage, V_{oc} = 0.04731 V, a fill factor, FF=0.551 and an efficiency, η=0.531 %. They were recommended for diode applications.

Keywords: FTO; titanium dioxide; refractive indices; solution technique; characterization.

INTRODUCTION

The study of TiO_2 semi conducting thin films is being pursued with an increasing interest on the account of their proven and potential applications in many semiconductor devices [12]. Although it has been one of the most studied oxides, still a lot remains to be investigated. Its applications have been met because of its understood working physics and its role in device applications. Such applications include photo induced water splitting, dye synthesized solar cells, gas sensing, and in display devices [7]. The development of new devices using titanium oxide relies on the working physics principles and therefore, any blend composites and advanced materials outside titanium oxide has its modification of mechanical, electrical, optical and thermal properties of thin films based on titanium dioxide so as to fulfil any desired demand for improved industries applications [10]. Currently, a number of investigations have been reported in literature on the electrical and optical properties of titanium oxide because much interest is geared towards the production of inexpensive thin films for various applications including solar cell applications. Titanium dioxide exhibit varying semiconducting characteristics of many thin films that may include high resistivity [11], heat reflectivity [13], catalytic properties [2], photo thermal conductivity [14] and diode characteristics [15] among others [8, 9, 3, 6].

METHODOLOGY

Reagents and Apparatus. The following reagents were used: PVA, distilled water, $ZnCl_2$, NH_3, and NH_4Cl_4 among the common laboratory devices and apparatus, like an electronic thermometer, clean glass slides, cleaned and dried beaker, and measuring cylinders.

Preparation of precursor solutions. The PVA solution was prepared by adding 900 ml of distilled water to 1.8 g of solid PVA and stirred at 360 K for 1 hr [11] and left to age until its temperature dropped to room temperature.

Experimental Procedure. Chemical bath technique was used for the preparation of the TiO_2 thin films in the presence of the PVA matrix in the fol-

lowing order. The bath was composed of 12 ml of 1 M $ZnCl_2$, 12 ml of 1 M NH_4Cl_4, 12 ml of 10 M NH_3 and 13 ml of PVA solution mixed in that order in 100 ml cleaned and dried beaker. After aging, clean glass slides were inserted almost vertically into the solution and allowed to proceed for 3 hrs at a constant temperature of 340 K.

Post Deposition Treatment. The growth process was allowed to proceed at constant temperature and the duration for all the films was maintained to be the same. Then the films were removed, cleaned, and dried. They were finally annealed in an argon oven for 1 hr before characterizing.

Film Characterization. A Spectrophotometer at normal incident of light in the wavelength range of 300–2000 nm was used. Absorption and transmittance spectra, refractive indices, and optical band gaps of the samples were determined.

Solar Cell fabrication. A solar cell consisting of Au/TiO_2/SnS/Au was fabricated. Using optimized TiO_2 thin films with transmittance of about 62%, sheet resistivity of 13.04 Ω/m and band gap of 3.16±0.05 eV, SnS with average absorbance of about 46 % sheet resistivity of 2.46±0.12×105 Ωcm and a band energy gap of 1.25±0.12 eV was used as an absorber layer. Gold conductive paste was used as electrical contacts.

RESULTS AND DISCUSSION

As an optical property, radiation transmittance through a thin film is described as how effective radiant energy is transmitted. That is why it is taken as the fraction of incident electromagnetic power that is transmitted through a sample or as the ratio of the transmitted to incident electric field [15]. This sets a basis in that a material's internal transmittance refers to energy loss by absorption. In this work, a direct measurement by a spectrophotometer was used to obtain transmittance and reflectance. It was then used to determine absorbance for both annealed thin films. Transmittance and absorbance data was represented in Figures 1 and Figure 2 for annealed TiO_2 thin films 250 °C.

In the Figure 1, transmittance in TiO_2 thin films increased with increase in wavelength in the range of 300 – 2000 nm where it can be observed that all TiO_2 thin films had a higher transmittance in the NIR region compared to VIS region. It is believed that an increase in crystallinity implied uniformity of a thin film since growth of crystal has a direct effect on transmittance [9].

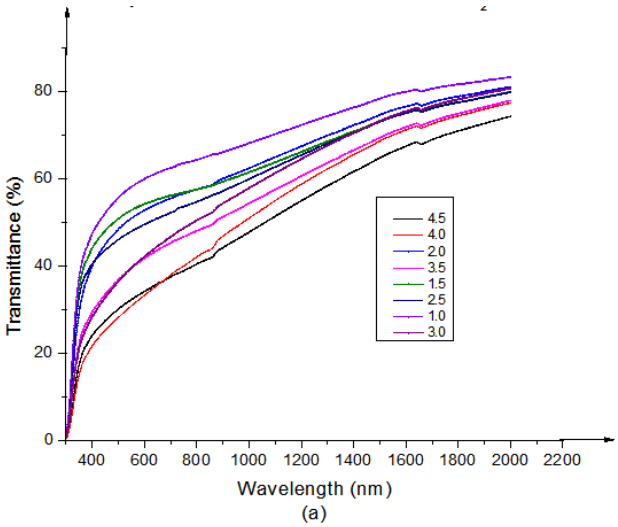

Figure 1 – Transmittance curve of annealed TiO_2 films at 250 °C

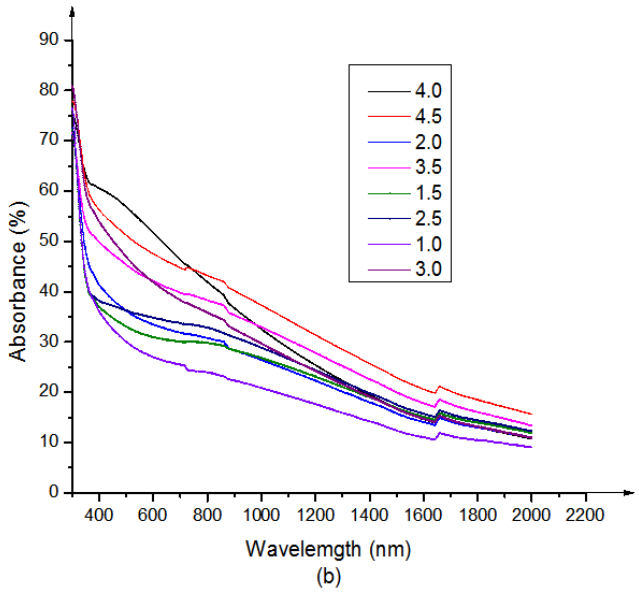

Figure 2 – Absorbance curve of annealed TiO_2 films at 250 °C

In the Figure 2, there was a significant decrease in absorbance with the increase in wavelength. TiO_2 films were either more transparent or more reflective at higher wavelengths as compared to lower wavelengths. This was attributed to be due to the nature of the grain size variation in relation to the wavelength of the photon energy. A comparison was made for transmittance, reflectance, and absorbance and the results were represented in Table 1.

Table 1 – Transmittance, reflectance, and absorbencies of TiO_2 thin films

Time (minutes)	1.0	1.5	2.0	2.5	3.0	3.5	4.0	4.5
Transmittance (%)	62.0	56.0	55.0	52.8	47.0	44.5	40.9	38.4
Reflectance (%)	12.5	13.8	13.9	14.3	15.0	16.0	17.2	18.0
Absorbance (%)	25.5	30.2	31.1	32.9	38.0	39.5	42.9	43.6

In thin films, annealing is taken as heat treatment that alters the physical and sometimes the chemical properties of a thin film. It is intended to increase or decrease or change or fine tune the thin film's intrinsic and extrinsic parameters to make it more or less workable or useful. It involves heating a material above its re-crystallization temperature or maintaining a suitable temperature, and then cooling it. In the annealing process, atoms migrate within the crystal lattice causing the number of dislocations to decreases [14]. Material annealing therefore can lead to phase transitions, re-crystallization, and homogenization, relaxation of internal stresses and re-arrangement of defects among other effects [15, 10] depending significantly on its kinetics, the rate of heating and cooling and the time of exposure at a given temperature.

In Figure 3, the thin films were annealed thin films of TiO_2 at 300 °C. They exhibited a transmittance that increased with increase in wavelength. However, a slight reduction of transmittance in the annealed thin film samples as opposed to as-deposited ones.

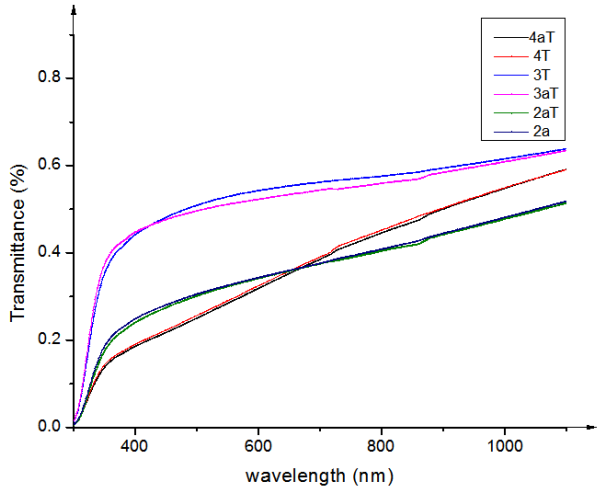

Figure 3 – Transmittance curve of annealed TiO_2 thin films at 300 °C

This was attributed to heat treatment which may have caused film surface changes and may have enhancing more light trapping or reflectance or absorbance [10].

Energy Band Gap

A band gap is a unique quality in thin films. When atoms come together to form a solid, their valence electrons interact using Coulomb forces [10]. The atoms feel the electric field produced by their own nucleus and that of the other atoms. As a result, two specific Quantum-Mechanical Effects takes place: through Heisenberg's uncertainty principle, the constraining of electrons to a small volume raises their energy. This is called promotion. By Pauli Exclusion Principle, which a number of electrons are limited to have the same property. In all these two effects, the valence electrons of atoms form wide valence bands when they form a solid. These bands get separated by gaps in which electrons do not exist in these gaps [8]. Therefore the term "band gap" refers to the energy difference between the top of the valence band to the bottom of the conduction band as depicted by Figure 4.

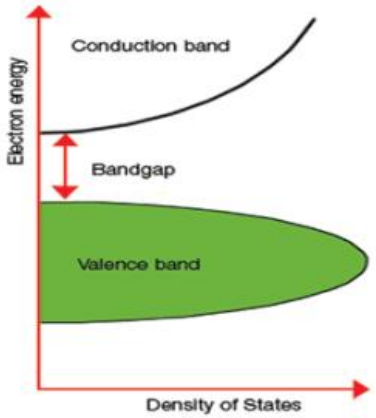

Figure 4 – Bloch equations Relation representing Band gap with density of states in semiconductor using [11]

Through this gap, electrons are able to jump from one band to another. In order for an electron to jump from a valence band to a conduction band, it requires specific minimum amount of energy for the transition to take place (*the band gap energy*). Band gaps of materials is important in the semiconductors, nano-material and solar technology.

In this work, the energy band gaps were determined using the semiconductor Bloch equations through simulations of transmittance data and extrapolating the linear portions of the plots $(\propto h\nu)^2$ against hν to where $(\propto h\nu)^2 = 0$. The obtained value was through extrapolating the line that cuts energy (*hν*) axis as depicted in Figure 5.

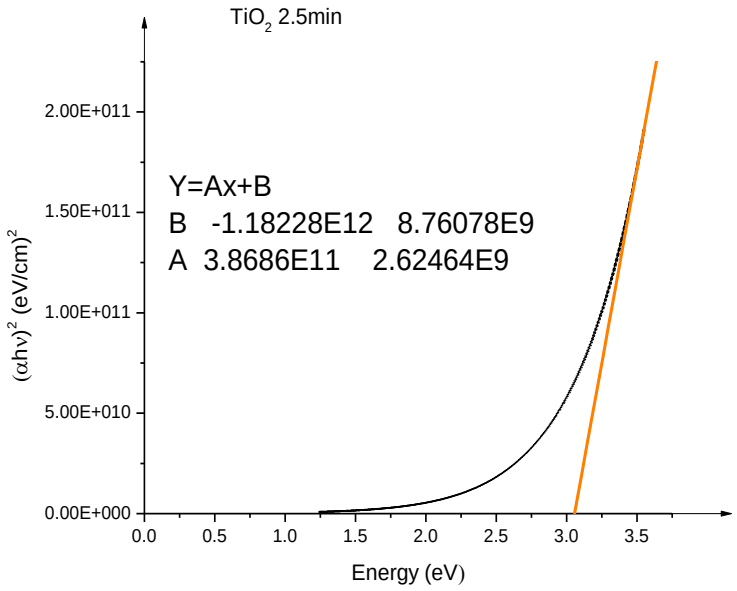

Figure 5 – TiO_2 energy band gap using extrapolation method

Further, the various band gaps were tabulated in Table 2 and Table 3 for different deposition times for both as-deposited and annealed TiO_2 thin films.

Table 2 – Band gaps of TiO_2 films deposited for different durations

Time (minutes)	1.0	1.5	2.0	2.5	3.0	3.5	4.0	4.5
Thickness (nm)	51.02±0.15	55.20±0.17	56.81±0.17	56.89±0.17	57.12±0.17	57.93±0.17	66.89±0.20	69.48±0.20
Eg eV (Annealed)	3.16±0.05	3.14±0.03	3.06±0.03	3.06±0.06	3.02±0.03	2.99±0.04	2.78±0.03	2.76±0.02
Eg eV (As-deposited)	3.32±0.05	3.20±0.03	3.11±0.03	3.09±0.08	3.08±0.03	3.00±0.04	2.86±0.03	2.79±0.02

Table 3 – Sheet resistivity and conductivity

Spray time (minutes)	Resistivity ,ρ (Ω/m)	Conductivity, σ (S/m)
1.0	13.54±0.095	7.386 x 10-3
1.5	14.46±0.101	6.916 x 10-3
2.0	14.36±0.099	6.963 x 10-3
2.5	16.47±0.115	6.071 x 10-3
3.0	16.56±0.115	6.039 x 10-3
3.5	17.03±0.119	5.871 x 10-3
4.0	17.14±0.120	5.834 x 10-3
4.5	17.27±0.209	5.579 x 10-3

In the 300–2000 nm wavelength region, the absorption coefficient, 'α' was derived from the expression [12]:

$$\alpha = \alpha_o \exp\left(\frac{h\nu}{\Delta E}\right) \quad (1)$$

Band gap and the energy offset was based on a simple assumed relation of atoms as $A_{1-x}B_x$. The band gap was then calculated by the formulae [11, 1]:

$$E_{g,X}^{AB} = E_{g,X}^{B}(1-x) + E_{g,X}^{A} + C_{g,X}(1-x)x \quad (2)$$

$$E_{g,\Gamma}^{AB} = E_{g,\Gamma}^{A}(1-x) + E_{g,\Gamma}^{B} + C_{g,\Gamma}(1-x)x \quad (3)$$

$$E_{g}^{AB} = \min\left(E_{g,X}^{AB}; E_{g,\Gamma}^{AB}\right) \quad (4)$$

where the bowing parameters, $C_g\Gamma$, C_g and $C_g x$ were used as reference in one-valley band gap fit.

The resulting combined values were obtained from the expressed [2]:

$$E_g^{AB} = E_g^A(1-x) + E_g^B + C_g(1-x)x \quad (5)$$

Refractive Index

In this work, refractive index was obtained using the standard Swanepoel's method instead of the Swanepoel's method that involves drawing envelopes connecting the extreme points of the interference fringes appearing in the spectrum from [11]:

$$n = \sqrt{N_1 + \sqrt{(N_1^2 - s^2)}}, \quad (6)$$

$$\text{where } N_1 = \frac{2s}{t_m} + \frac{s^2+1}{2} \quad (7)$$

where *N* is the refractive index, tm is the minima of the interference fringes and 's' is the refractive index of the substrate.

Refractive index trend also followed the Sellmeier relation [9]:

$$n^2 = A + \sum_j \frac{B_j \lambda^2}{\lambda^2 - C_{oj}} \quad (8)$$

with Sellmeier model's constants and film thickness consistent till a small value of Mean Square Error (MSE) was obtained.

Refractive indices was also analyzed and deduced by scout software simulation as fitted by experimental data. The values obtained were in the range of 2.2–2.5 in the visible range. Therefore, Sellmeier model gives an empirical formula. However, similar relations for the refractive index that agreed with experimental and simulated data included the Cauchy's dispersion relation expressed as [14]:

$$n = 1.489 + \frac{3.23\times10^3}{\lambda^2}, \quad (9)$$

Resulting in an extinction coefficient of:

$$k = 6.89\times10^{-4} + 0.012\exp^{[3.05(\frac{1240}{\lambda}-4.342)]} \quad (10)$$

Electrical properties

One of the subatomic particles of an atom is the electron. Electrons carry a negative electrostatic charge and under certain conditions can move from atom to atom in a random motion unless a force causes the electrons to move in one direction [3]. Directional movement of electrons due to an electromotive force is what is known as electricity and is used to define conductivity as a measure of how well a material accommodates the movement of an electric charge or the ratio of the current density to the electric field strength. Conductivity values are often reported as percent in IACS where IACS is an acronym for International Annealed Copper Standard, which was established by the 1913 International Electrochemical Commission [6].

Optimized sheet resistivity of TiO2 thin films deposited on FTO glass substrates was approximated to ranged between 13.54±0.095 Ω/m to 17.27±0.209 Ω/m as measured using SRM-232 surface resistivity meter. Further analysis was tabulated Table 3 and Figure 6. The observations were attributed to an increase of the grain boundaries within the crystals [13].

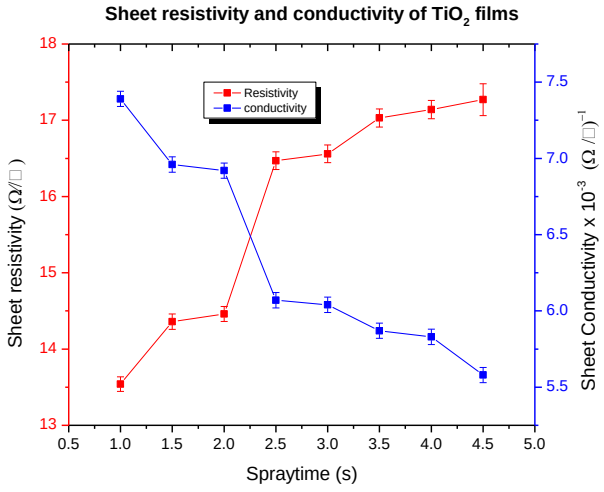

Figure 6 – Relationship of Sheet resistivity and conductivity of TiO_2 films

Solar Cell Parameters

A solar simulator was used to determine the Au/TiO2-SnS/Au solar cell's I–V characteristics and the results presented in Table 3. The solar cell parameters obtained from the I–V measurements included short circuit current (I_{sc}), open circuit voltage (V_{oc}), fill factor (FF), current at maximum power output (I_{max}), voltage at maximum power output (V_{max}) and conversion efficiency (η). Fill factor is a measure of the quality of a cell and therefore a large fill factor of 1 or very close to 1 is desirable and it corresponds to I-V sweep that is more square-like where typical fill factors ranges from 0.50 to 0.82 [5]. The fabricated photovoltaic cell had a short circuit current, I_{sc}=0.002445 A, open voltage, V_{oc}=0.04731 V, a fill factor, FF=0.551 and an efficiency, η=0.531 % as shown in Table 4.

Table 4 – Solar Cell parameters

Cell parameters	Value of parameter/unit
I_{sc}	2.445 mA
V_{oc}	47.31 mV
I_{max}	2.14 mA
V_{max}	26.071 mV
P_{max}	0.063744 mW
FF	0.551
η	0.531

The square-like nature of the I–V curve was used to obtain the fill factor of 0.551, maximum power of 0.637 mW. It was concluded that the fabricated p-n junction resulted in the photovoltaic effect as depicted by figure 7.

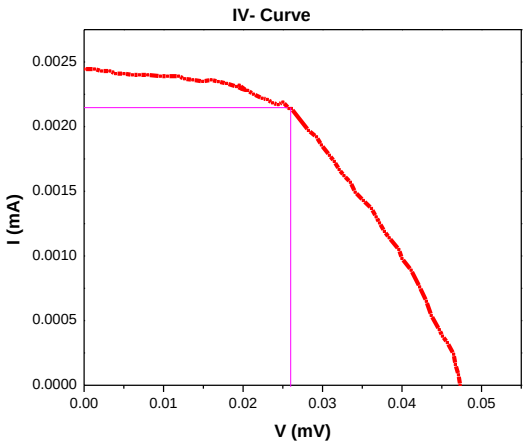

Figure 7 – Solar cell I-V curve characteristics

CONCLUSIONS

In this study, TiO_2 thin films were synthesized using chemical bath deposition. Their electrical and optical properties were examined. The thin films had refractive indices in the range of 2.2–2.5 in the visible range spectra and sheet resistivity ranged between 13.54±0.095 Ω/m to 17.27±0.209 Ω/m. The fabricated solar cell had a short circuit current, I_{sc} = 0.002445 A, open voltage, V_{oc}=0.04731 V, a fill factor, FF=0.551 and an efficiency, η=0.531 %. The thin films were recommended for solar cell and diode applications.

ACKNOWLEDGEMENTS

The authors thank department of Material Science in the University of Nairobi for allowing us use the spectrophotometer for transmission and absorbance measurements and the department of Mathematics and Physics of Technical University of Mombasa.

REFERENCES

1. Anpo, M. (2000). Use of visible light. Second-generation titanium oxide photocatalysts prepared by the application of an advanced metal ion-implantation method. *Pure and Applied Chemistry, 72*(9), 1787–1792. doi: 10.1351/pac200072091787
2. Hass, G. (1952). Preparation, properties and optical applications of thin films of titanium dioxide. *Vacuum, 2*(4), 331–345. doi: 10.1016/0042-207x(52)93783-4
3. Huang, D., Xiao, Z.-D., Gu, J.-H., Huang, N.-P., & Yuan, C.-W. (1997). TiO2 thin films formation on industrial glass through self-assembly processing. *Thin Solid Films, 305*(1-2), 110–115. doi: 10.1016/s0040-6090(97)00202-2
4. Justicia, I., Ordejón, P., Canto, G., Mozos, J. L., Fraxedas, J., Battiston, G. A., ... & Figueras, A. (2002). Designed Self-Doped Titanium Oxide Thin Films for Efficient Visible-Light Photocatalysis.

Advanced Materials, 14(19), 1399-1402. doi: 10.1002/1521-4095(20021002)14:19%3C1399::AID-ADMA1399%3E3.0.CO;2-C

5. Löbl, P., Huppertz, M., & Mergel, D. (1994). Nucleation and growth in TiO2 films prepared by sputtering and evaporation. *Thin Solid Films, 251*(1), 72–79. doi: 10.1016/0040-6090(94)90843-5
6. Lu, J.-P., Wang, J., & Raj, R. (1991). Solution precursor chemical vapor deposition of titanium oxide thin films. *Thin Solid Films, 204*(1), L13–L17. doi: 10.1016/0040-6090(91)90488-j
7. Luu, T. T., Garg, M., Kruchinin, S. Y., Moulet, A., Hassan, M. T., & Goulielmakis, E. (2015). Extreme ultraviolet high-harmonic spectroscopy of solids. *Nature, 521*(7553), 498–502. doi: 10.1038/nature14456
8. Martin, N., Rousselot, C., Rondot, D., Palmino, F., & Mercier, R. (1997). Microstructure modification of amorphous titanium oxide thin films during annealing treatment. *Thin Solid Films, 300*(1-2), 113–121. doi: 10.1016/s0040-6090(96)09510-7
9. Martin, N., Rousselot, C., Savall, C., & Palmino, F. (1996). Characterizations of titanium oxide films prepared by radio frequency magnetron sputtering. *Thin Solid Films, 287*(1-2), 154–163. doi: 10.1016/s0040-6090(96)08782-2
10. Negishi, N., Takeuchi, K., & Ibusuki, T. (1997). The surface structure of titanium dioxide thin film photocatalyst. *Applied Surface Science, 121-122*, 417–420. doi: 10.1016/s0169-4332(97)00349-8
11. Ohsuku, T., & Hirai, T. (1982). An electrochromic display based on titanium dioxide. *Electrochimica Acta, 27*(9), 1263–1266. doi: 10.1016/0013-4686(82)80146-1
12. Poelman, D., & Smet, P. F. (2003). Methods for the determination of the optical constants of thin films from single transmission measurements: a critical review. *Journal of Physics D: Applied Physics, 36*(15), 1850–1857. doi: 10.1088/0022-3727/36/15/316
13. Ritala, M., Rahtu, A., Leskela, M., & Kukli, K. (2003). *Method for growing thin oxide films* (US Patent No US6632279B1). Retrieved from https://patents.google.com/patent/US6632279
14. Vampa, G., Hammond, T. J., Thiré, N., Schmidt, B. E., Légaré, F., McDonald, C. R., … Corkum, P. B. (2015). Linking high harmonics from gases and solids. *Nature, 522*(7557), 462–464. doi: 10.1038/nature14517
15. Wu, M., Ghimire, S., Reis, D. A., Schafer, K. J., & Gaarde, M. B. (2015). High-harmonic generation from Bloch electrons in solids. *Physical Review A, 91*(4). doi: 10.1103/physreva.91.043839